A Method for the Determination of Shape Actuator Capabilities Envelopes in 20-High Cluster Mills

Mark E. Zipf
Tenova I2S (I2S, LLC)
475 Main St.
Yalesville, CT 06492
Tel: (203)-265-5684
E-Mail: mzipf@i2s.com

Keywords: 20-High, Cluster Mill, Shape Actuators, Spatial Influence Functions, Parameter Identification, Modeling, Spatial Waveforms, Spatial Curvatures, Orthogonal Polynomials, Parametric Decomposition, Capabilities Envelope

ABSTRACT

The shape actuation characteristics of 4-high and 6-high mill arrangements are well understood and fairly intuitive. Unfortunately, these same characteristics of 20-high cluster mills are poorly understood and counter-intuitive. A method has been developed that combines the spatial influence functions of the multiple 20-high shape actuators and maps-out their combined capabilities, over the entire range of constrained actuation. Using an orthogonal polynomial based decomposing transformation, the results are plotted within a spatial curvature basis, from which the achievable shape adjustment curvatures form a closed region (an envelope). The extents of this envelope are determined by image processing vertices methods.

1.0 – INTRODUCTION

When considering methods of describing the shape actuation characteristics of rolling mills, it is possible to depict the extent of a mill's capabilities as a continuous, closed region of a linearly algebraic vector space, whose basis set (orthogonal directions) is formed over the field of ordered transverse spatial curvatures (i.e., 1st order : slope, 2nd : parabolic, 3rd : cubic, etc.). The examination of this region is often carried-out through 2-dimensional "slicing", forming cross-section planes typically between adjacent orders of curvature (2nd & 4th orders or 4th and 6th orders, etc.). The closed-region within the plane, specifically defines the nature and extent of contribution of spatial curvature orders that can be provided by the shape actuators [1,2].

The idea is to decompose the complexities of the rolled shape's spatial waveform (stress pattern across the strip) resulting from a given shape actuator system setting, into its simplified curvature constituents (a collection of ordered spatial curvatures). For that specific shape actuator setting, this collection of curvatures forms a point (described by a unique vector) in the above mentioned vector space. By evaluating the rolled shape curvatures over the entire range of shape actuator settings (including the presence of physical and operational constraints), the resulting points (vectors) will map-out a region in the space. A bounding, piece-wise continuous, closed curve / surface can then be drawn along the extremity of the collection of plotted points, forming a closed region. This bounding curve / surface functions as an over-containing envelope of the region and thereby defines the extent of the mill's shape actuation capabilities. We will term this envelope as the Shape Actuation Capabilities Envelope (SACE). Figure 1 provides a conceptual illustration of the regions / envelopes characterizing the SACEs of contemporary mills.

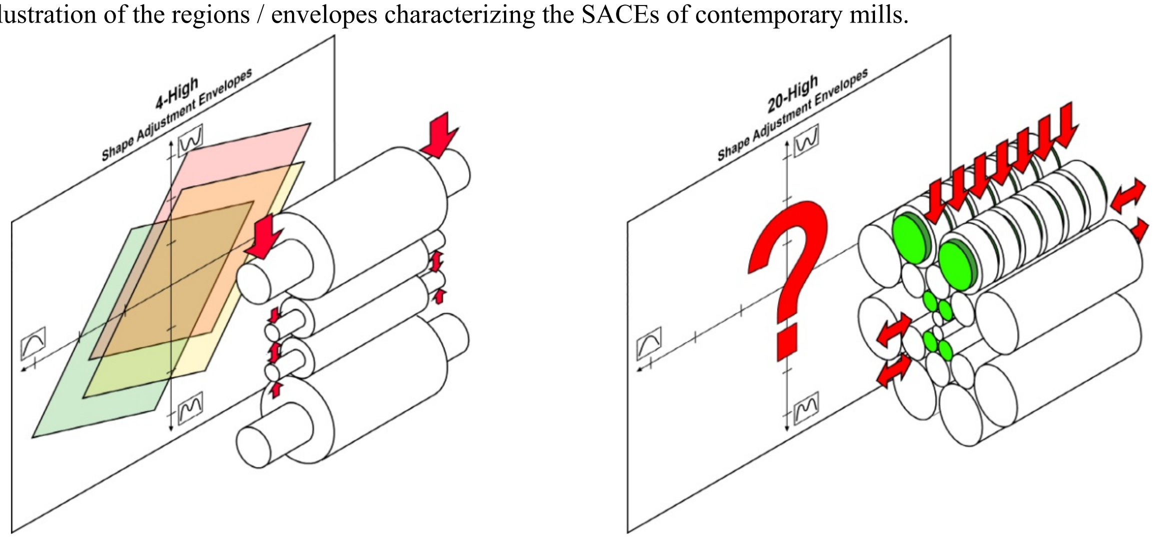

Figure 1 – Conceptual illustrations of the regions / envelopes characterizing the shape actuation capabilities (SACEs) of a vertical stack 4-high and a 20-high cluster mill.

As noted in Figure 1, the regions of shape actuation capability for 4-high (and 6-high) vertical stack arrangements are well defined [1,2]. Unfortunately, the nature of these capability regions for 20-high cluster mills, are poorly understood.

This work involves the development of a method to determine the capabilities envelopes (SACEs) of 20-high cluster mills, by employing a fully adapting matrix model (formed from modeling and empirical studies [3]) and a compact transformation technique to form a computationally efficient means of determining the rolled shape waveform's spatial curvature constituents, for a given actuator setting, as a unique vector residing in the curvature vector space. By evaluating the entire range of the constrained actuation settings, it is possible to map-out the entire set of vectors (points) describing the rolled shapes amenable to the actuation system.

Through continuity, this set of vectors (spatial curvature constituents of the actuated / rolled shapes) spans a continuous region of the curvature vector space, that can be over-contained / bounded by closed, piece-wise continuous curve / surface. This curve can be determined by using image processing edge detection methods [4], to identify the region's extremities and the associated bounding curve segments. For a particular condition (strip width, thickness, yield stress, separating force, etc.), the resulting curve / surface forms an envelope that describes the extent of the actuation's shape adjustment capabilities, the SACE for that instance and situation.

Examining the nature and relationships of these envelopes for a variety of different operating conditions (e.g., over the pass-to-pass progression), provides the ability to define the range of available shape actuation corrections for given situations. This provides a much needed insight into the available pass schedules, shape targets and roll cluster set-ups that can be accommodated by the mill.

The remainder of this paper provides a description of this method. Section 2 provides an overview of the 20-high mill shape actuation and a method for describing its shape actuation response characteristics, followed by a mathematical model and strategy for identifying the model's parameters. Section 3 presents a method for decomposing the shape actuator induced spatial waveforms (patterns) into their spatial curvature constituents and resulting vector representations. Section 4 presents a method for evaluating the entire range of constrained actuator settings to determine the mill's Shape Actuation Capabilities Envelope (SACE).

2.0 – 20-HIGH CLUSTER MILL SHAPE ACTUATION

20-High Cluster Mills adjust the strip's shape (stress pattern) by coordinating a set of actuators to modify the applied transverse pressure distribution, thereby altering the localized strip elongation / strain and resulting transverse stress / tension distribution of the rolled strip. A common actuation configuration [5], is shown in Figure 2.

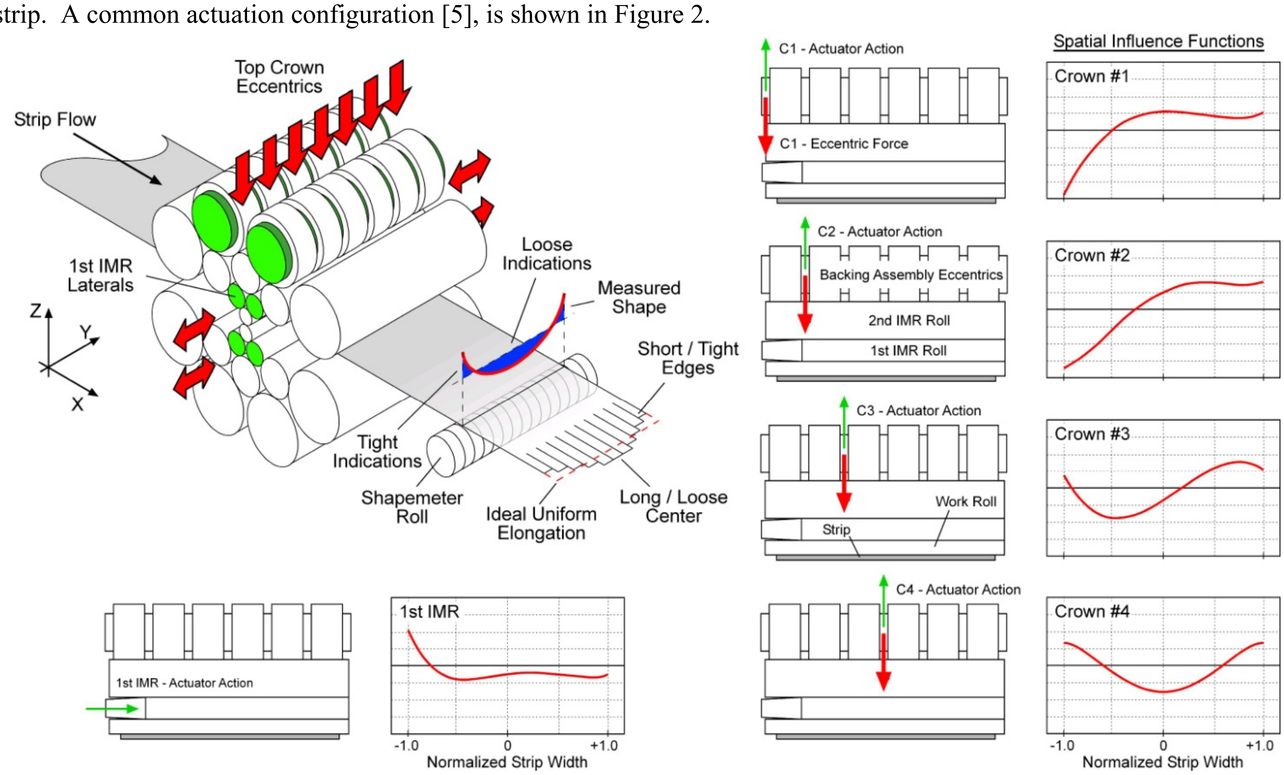

Figure 2 – Illustration of cluster mill shape actuation systems and their associated transverse spatial influence functions.

Each actuator induces a unique transverse stress adjustment pattern / reaction that can be characterized by a continuous spatial influence function (waveform). These spatial influences are not localized to the vicinity of the actuator's physical location, but span the strip width, due to the manner in which the roll cluster mechanically reacts / deforms and subsequently distributes the actuator forces to the roll bite. The actuator influence functions are non-linear and have highly coupled interactions, that by definition have a zero mean so as to be non-interactive with the thickness control system (AGC). As shown in Figure 3, the behavior of these functions vary greatly over the material characteristics, operating conditions and mill set-up philosophy.

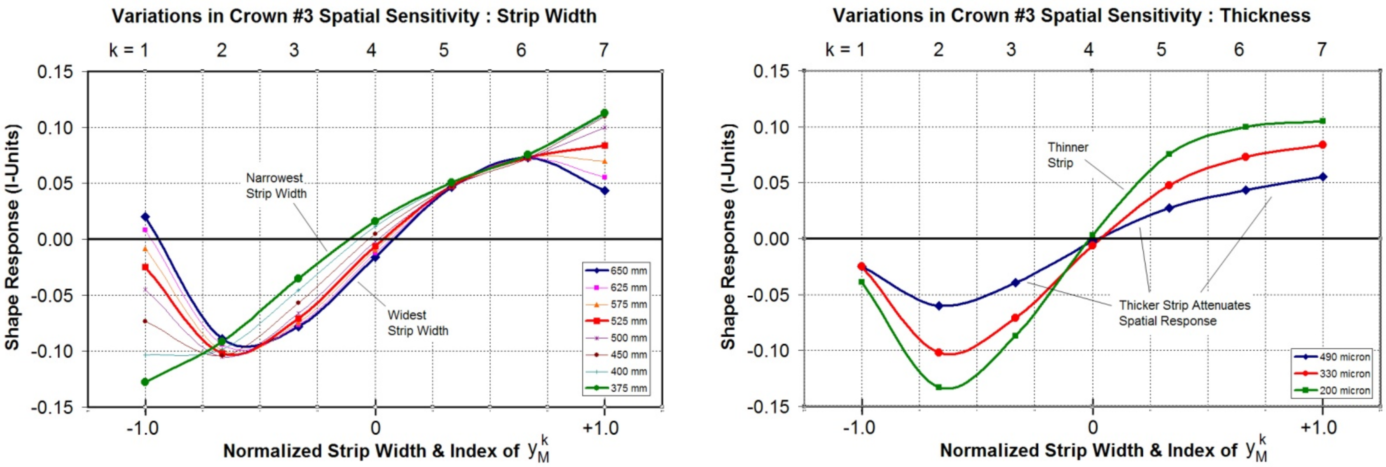

Figure 3 – Illustration of cluster mill shape actuation including transverse spatial influence functions.

2.1 – System Modeling

It is possible to describe the overall mill's influences on the rolled shape / stress pattern through analytic models that consider the contributions of various components (i.e., incoming strip shape, roll cluster set-up, actuation, etc.). The transverse distribution of stress (shape) within the strip, from an arbitrary contributing component, is described by a spatial waveform or pattern (i.e., a continuous spatial influence function evolving over the transverse space of the strip's width). The linear algebraic model is based on formulating the rolled exit strip shape's waveform pattern as the discrete, spatially aligned superposition of the contributors [6,7,8,9].

$$\mathbf{S}_T\left(y_M\right) \sim \mathbf{S}\left(y_M\right) = \mathbf{S}_0\left(y_M\right) + \mathbf{S}_R\left(y_M\right) + \mathbf{S}_A\left(y_M\right) \qquad \text{Discrete Spatial Function} \tag{1}$$

were these components are the discrete, spatial representations of these transverse shape / stress waveform patterns, given by:

$\mathbf{S}(y_M)$ $\triangleq$ Rolled / exist strip shape vector (stress pattern) produced by the mill, given by:

$$\mathbf{S}_A\left(y_M\right) = \left[S_A\left(y_M^0\right) \quad S_A\left(y_M^1\right) \quad \cdots \quad S_A\left(y_M^{M-1}\right)\right]^T \tag{2}$$

The elements of this vector are the stress amplitudes at the corresponding transverse locations of y_M.

$\mathbf{S}_T(y_M)$ $\triangleq$ Shape target vector, indicating the desired shape of the rolled / exit strip.

$\mathbf{S}_0(y_M)$ $\triangleq$ Incoming strip shape vector. This component is static for the evaluated situation.

$\mathbf{S}_R(y_M)$ $\triangleq$ Exit strip shape contribution vector formed by the natural mechanical deformation characteristics of the mill, and is based on a combination of material geometry and yield stress, applied separating force, roll cluster set-up of roll profiles and tapers, roll cluster flexibility [10], etc.. This component is static and can not be modified during on-line / rolling operations.

$\mathbf{S}_A(y_M)$ $\triangleq$ Exit strip shape contribution vector induced by the Top Crown Eccentrics and 1st IMR laterals, as transmitted / distributed to the roll bite through the roll cluster's mechanical characteristics (which function as a form of spatial filter). This component is dynamic and can be modified / adjusted during on-line / rolling operations. The nature of the actuation's spatial influence varies over the operating conditions, requiring a degree of adaptation to describe the full range of rolling conditions.

The discrete spatial variable, y_M, is an M dimensional set of uniformly distributed locations across the strip width, W, which have been mapped to the normalized domain interval [-W/2, +W/2] $\rightarrow$ [-1, 1] of a Sobolev space.

$$y_M = \left\{y_M^0, y_M^1, \cdots, y_M^{M-1}\right\} \qquad \text{with the requirement of:} \quad y_M^0 = -1 \text{ and } y_M^{M-1} = +1 \tag{3}$$

In this linear algebraic framework, the spatial waveform characteristics of the mill's transmission of the shape actuator settings is provided through a matrix, $\mathbf{G}_M \in \Re^{MxN}$, whose columns are evaluations of the individual actuator's spatial influence at the sampling grid associated with y_M. This representation provides a specific definition of the actuator's dynamic changes in the shape, $\mathbf{S}_A(y_M)$:

$$\mathbf{S}_A\left(y_M\right) = \mathbf{G}_M \mathbf{A} \tag{4}$$

where $\mathbf{A} \in \Re^N$ is the actuation vector. The central relationship of Eq(1) becomes:

$$\mathbf{S}\left(y_M\right) = \mathbf{S}_0\left(y_M\right) + \mathbf{S}_R\left(y_M\right) + \mathbf{G}_M \mathbf{A} \tag{5}$$

Figure 4 shows the basic structure of a simple, computationally efficient, linear algebraic model based on a discrete spatial description (discrete sampling grid across the strip).

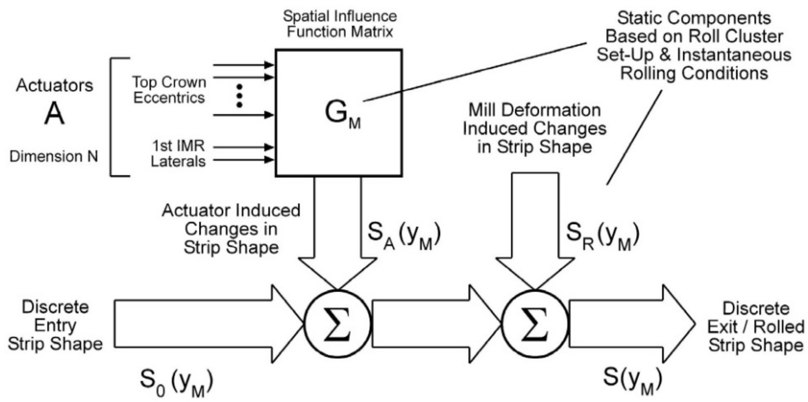

Figure 4 – Block diagram illustration showing the discrete spatial relationships of the modeled components of the rolled strip shape, including the shape actuation's transverse spatial influence functions and the roll cluster deformation contributions.

Together, the actuated dynamic component, $\mathbf{S}_A(y_M)$, and the static component, $\mathbf{S}_R(y_M)$, constitute the available degrees of freedom, both actively and as part of a process engineering design (i.e., the selection of the roll cluster set-up and the tuning of the pass schedule). The design of $\mathbf{S}_R(y_M)$ is complex "black art" that involves paying careful attention to the cluster's roll profiles and pass schedule, to program the progression of the separating force induced mill deformation over the pass-to-pass sequence. This is the subject of other discussions [21], and for this work, $\mathbf{S}_R(y_M)$, will be treated as a static vector having 2nd and 4th order spatial curvatures.

2.2 – Characterizing the Elements of the G_M Matrix

The internal arrangement of the $\mathbf{G}_M\mathbf{A}$ relationship is based on the column vector format of $\mathbf{G}_M$ and considers the rolled shape reaction, $\mathbf{S}_A(y_M)$ (spatial influence function), due to the operation of a single actuator, a_i.

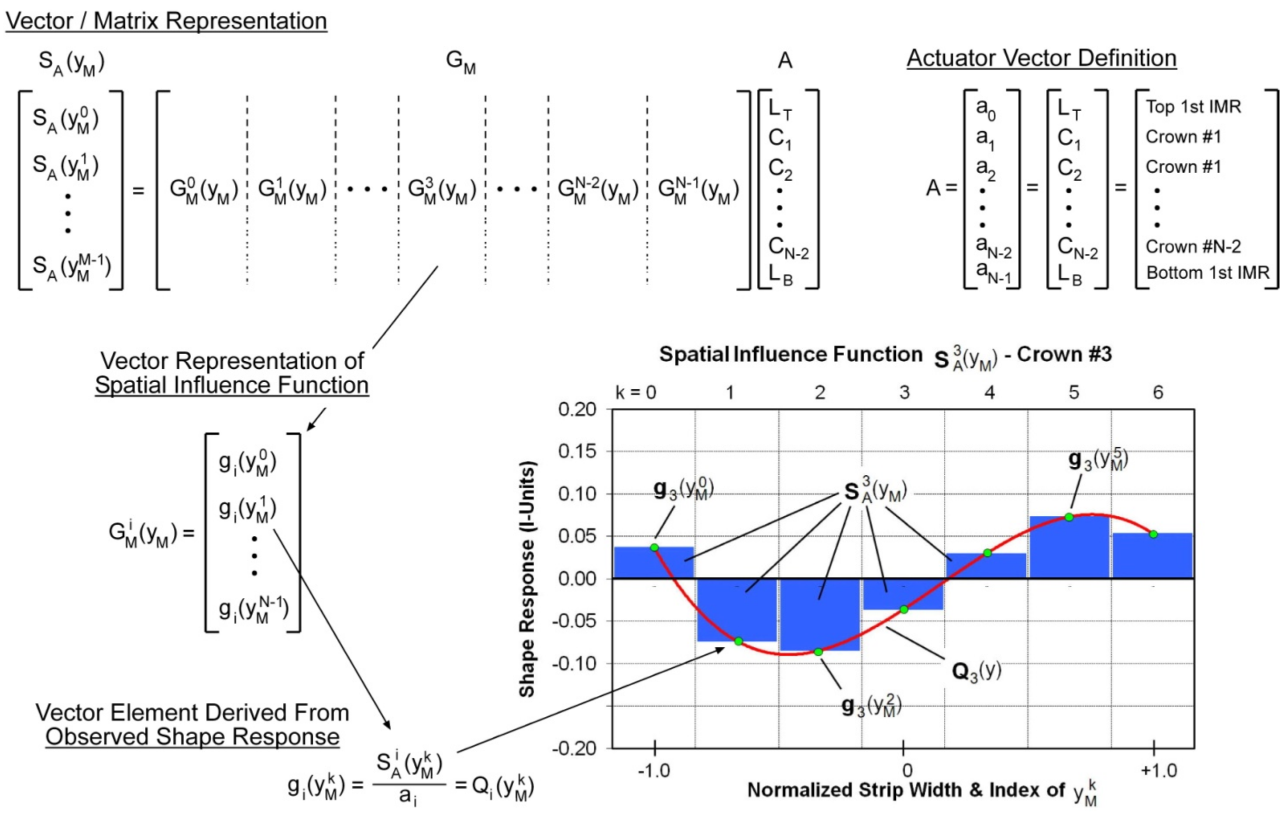

Figure 5 – Illustration showing the determination of a $\mathbf{G}_M$ column vector element from the evaluation of the spatial influence function of the associated actuator, along the transverse grid pattern defined by y_M.

Therefore, each column vector of $\mathbf{G}_M$ specifically defines the spatial influence of a unique / specific actuator. The elements of these column vectors are specifically located (through y_M) evaluations of a single actuator's spatial influence function along the transverse range of the strip width.

2.3 – Polynomial Representation of Spatial Influence Functions

Figure 5 shows that the elements of the vector representation of a spatial influence function can be determined through the evaluation of the polynomial $Q_i(y)$. The spatial influence functions are dominated by lower spatial frequency components, which can be described by low order polynomials that are continuous across the strip width (continuous in "y"). In general, the nature of the curvature and spatial frequency are described [9] by 8th order polynomials of the form:

$$Q_i(y) = \alpha_8^i y^8 + \alpha_7^i y^7 + \cdots + \alpha_2^i y^2 + \alpha_1^i y + \alpha_0^i \tag{6}$$

The coefficients are shown as constants, but they may also be complex functions related to the strip characteristics and operating conditions. The variability of the influence functions (as noted in Figure 3) can be accommodated through properly mapped adjustments of the coefficients (as discussed in Section 2.6).

2.4 – Parameter Identification of the Spatial Influence Function's Describing Polynomial

Parametric identification of the mill actuator spatial influence function's describing polynomials is provided by employing differential perturbation methods involving the transverse dynamic response characteristics of the rolled and measured exit strip shape to individual actuator excitation. Probative system identification signals involve low amplitude, bipolar, zero mean, colored noise waveforms designed to provide the necessary excitation of the individual actuators and to be easily deconvolved from the shape controller's actuator commands and from the resulting strip shape adjustments [11]. The signals are also designed to not affect the shape performance or distract the shape control system.

As shown in Figure 6, the probative signals are injected into the mill actuation to cause measured responses that represent the spatial influence function, $\overline{S_A}(y_S)$. These responses are combined to generate a high spatial frequency description of each actuator's spatial influence function, $S_A(y_S)$, at the resolution of the shapemeter measurements. A Least Squares fitting algorithm is used to form the polynomial representation, $Q_i(y)$.

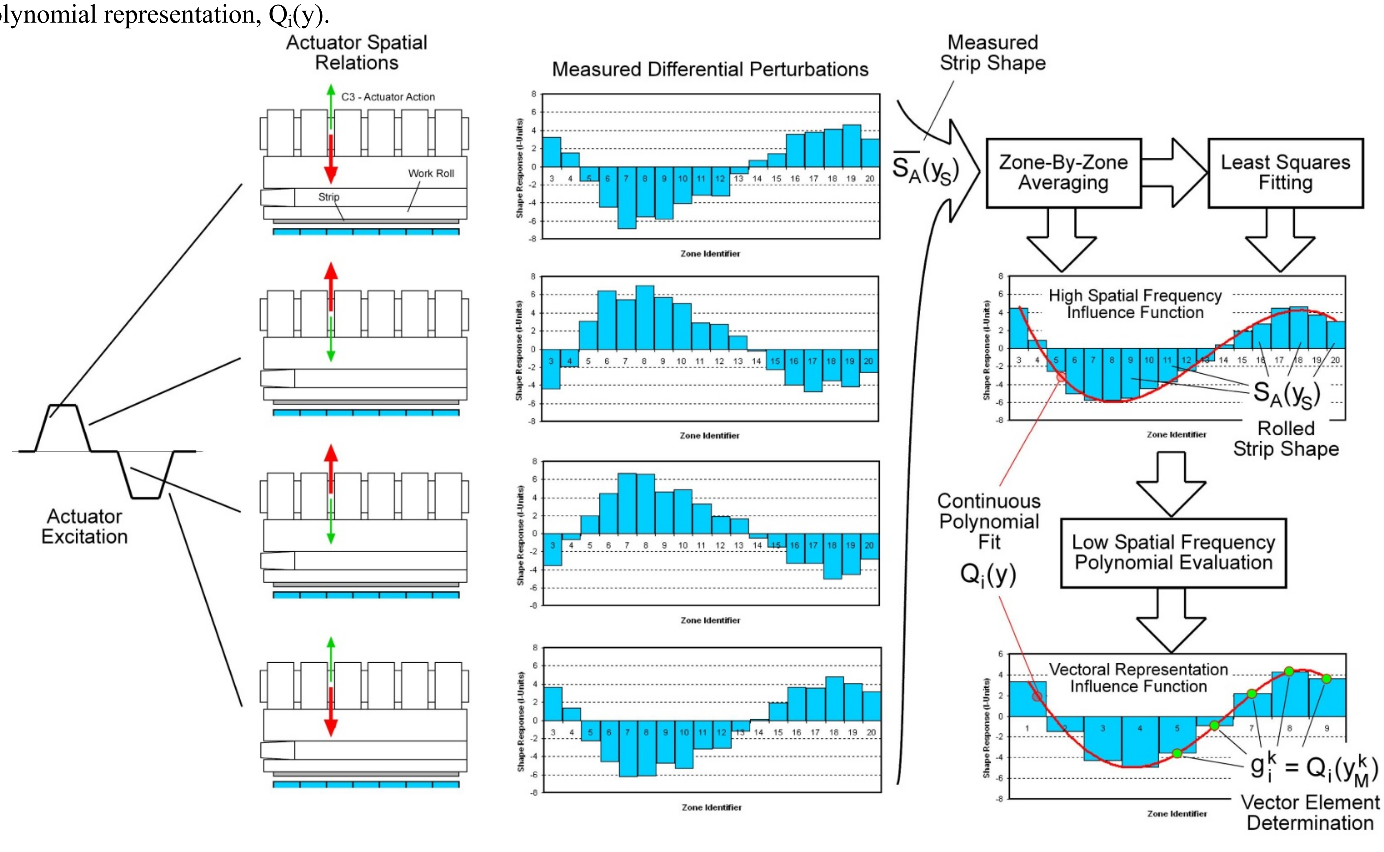

Figure 6 – Diagram showing the parametric identification method based on a least squares fit of high resolution measurements of the mill's / material's response to probative actuation signals

This form of parameter identification involves dove-tailing the on-line studies with the operational scheduling and immediate product mix of the mill, which may not cover the board range and variability of operating condition that are needed to fully describe the extent of the mill's capabilities. It is possible to expand the range of the studies through analytic models [12,13,14], that are also subjected to these probative actuator signals (in an off-line manner), to determine the spatial influence functions for operating conditions that are not immediately available to the on-line studies.

2.5 – Parameter Identification of the Elements of the G_M Matrix

Sections 2.2, 2.3 and 2.4, along with Figures 5 and 6, provide a framework and methodology for identifying the elements of the $\mathbf{G}_M$ matrix over the entire operating range of the mill and material product mix. As shown in Figure 6, this process involves probative measurement of the individual actuator's spatial influence function, and Least Squares fitting of the measured spatial waveform, to determine the polynomial representation, $Q_i(y)$. Figure 7 provides a block diagram illustration of this process.

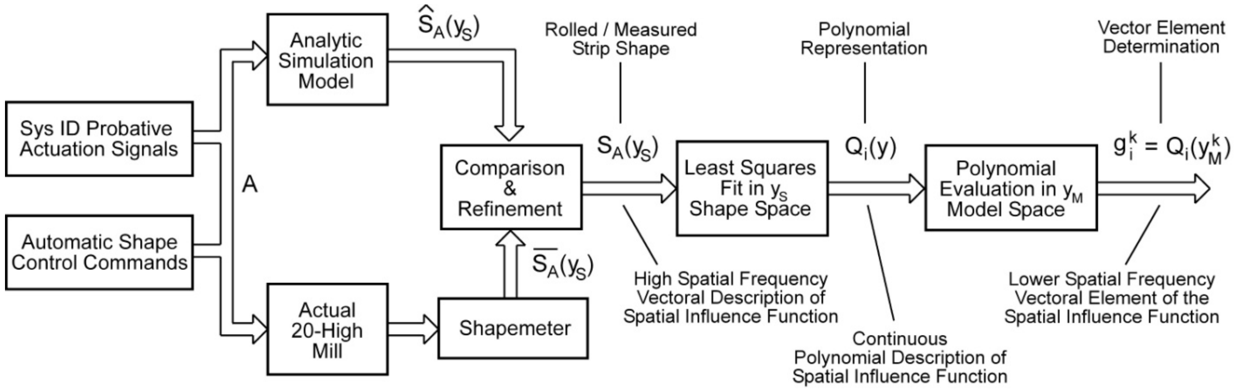

Figure 7 – Block diagram showing the process associated with the parameter identification of the elements of the GM matrix (spatial influence functions), through the evaluation of polynomial fits of the actual and / or simulated mill responses [12,13,14] to probative actuation signals.

The elements of the column vector, $\mathbf{G}_M^i(y_M)$, are determined by direct evaluation of the polynomial, $Q_i(y)$, at the specific discrete location, y_M^k, that corresponds to the vector element, $g_i(y_M^k)$, or:

$$g_i(y_M^k) = Q_i(y_M^k) \tag{7}$$

This process is continued as the overall product mix is rolled (on-line) or simulated (off-line), establishing a broad database of responses and identified parameters. Using Monte Carlo-like techniques, this database ultimately provides a sufficiently full population of all operational conditions considered. The evolution of this population allows the details of the spatial influence functions' variations due to material characteristics, operating conditions and mill set-up to be examined. This expanding (and overlapping) population also provides a refining quality to the modeled results.

2.6 – Multi-Variable Polynomial Description of the Spatial Influence Function Variability

As shown in Figure 3, the spatial influence functions vary primarily with the strip width and thickness (along with many other variables). This variability can be described (in a single degree of freedom / dimension) by the changes in the coefficients, α_j^i, of the polynomials, Q(y). These variations in the coefficients can be described by low order polynomials where the coefficients are separate functions associated with the strip characteristics and operating conditions. Consider the nature of the polynomial approximation to the Crown #3 spatial influence function with respect to changes in strip width (see Figure 3). Here, the coefficients of the polynomial, $Q_3(y)$, vary as a function of width:

$$Q_3(y,w) = \alpha_8^3(w)y^8 + \alpha_7^3(w)y^7 + \cdots + \alpha_2^3(w)y^2 + \alpha_1^3(w)y + \alpha_0^3(w) \tag{8}$$

The functional relationships of the coefficients themselves can be described by low order polynomials, where p = 0, 1, …, 8:

$$\alpha_p^3(w) = \beta_{p3}^3 w^3 + \beta_{p2}^3 w^2 + \beta_{p1}^3 w + \beta_{p0}^3 \tag{9}$$

Similar coefficient variation can be described for changes in material thickness, yield stress, and cluster flexibility [10]. The result is that each coefficient of $Q_3(y,\ldots)$ is a multi-dimensional surface (3 in this case) that comprehensively describes the reaction to all variability in the spatial influence function. Figure 8 provides an illustration of the 2 dimensional coefficient surface for the variations in width and thickness for the $\alpha_4^3(w,t)$ coefficient. Combining variations, the resulting polynomial description of Eq(6) becomes:

$$Q_i(y,w,t,\sigma_S) = \alpha_8^i(w,t,\sigma_S)y^8 + \alpha_7^i(w,t,\sigma_S)y^7 + \cdots + \alpha_2^i(w,t,\sigma_S)y^2 + \alpha_1^i(w,t,\sigma_S)y + \alpha_0^i(w,t,\sigma_S) \tag{10}$$

where the coefficients are multi-dimensional surfaces described by polynomial functions. The elements of the column vectors of the $\mathbf{G}_M$ are now given by:

$$g_i(y_M^k,w,t,\sigma_S) = Q_i(y_M^k,w,t,\sigma_S) \tag{11}$$

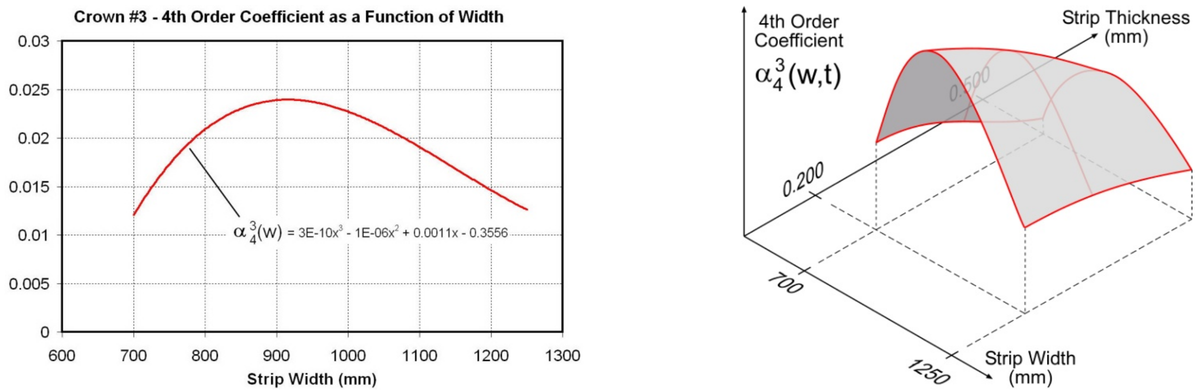

(a) (b)

Figure 8 – Illustrations of Crown #3's 4th order coefficient variations: a) Variation with respect to strip width, b) 2-Dimensional coefficient surface with respect to strip width and strip thickness.

3.0 – SPATIAL CURVATURE CHARACTERIZATION THROUGH PARAMETER DECOMPOSITION

The spatial waveform patterns of the strip shape components of Eqs(1) and Eq(5) (i.e., S_0, S_R, S_A) can be described by a simplifying vectoral distribution / spectrum of spatial curvatures [15,16,17,18]. An interesting Approximation Theory [18] approach uses an orthogonal polynomial basis to frame the description of the shape patterns / waveforms. Here, the spatial characteristics of the shape patterns / waveforms are described by the combination of orthogonal polynomial-based spatial curvatures.

3.1 – Spatial Waveform Approximation Using an Orthogonal Polynomial Basis

In the appropriate Sobolev space, the set of Gram orthogonal polynomials [15,16,17,19] form a complete basis set. Therefore, functions occurring in the continuous domain $-1 \le y \le 1$ can be expressed / approximated by the truncated expansion:

$$\mathbf{S}(y) = \sum_{i=1}^{N_p} \mathbf{\$}_S^i \, \mathbf{P}_i(y) \tag{12}$$

where

$P_i(y) \triangleq$ Gram polynomials

$\$_S^i \triangleq$ Coefficients indicating the contribution weighting of the individual polynomials

Np $\triangleq$ The desired cut-off in the degree / order of curvature used in making the approximation

The Gram polynomials are shown in Figure 9, while Figure 10 illustrates the nature of the weighted summation of Eq(12).

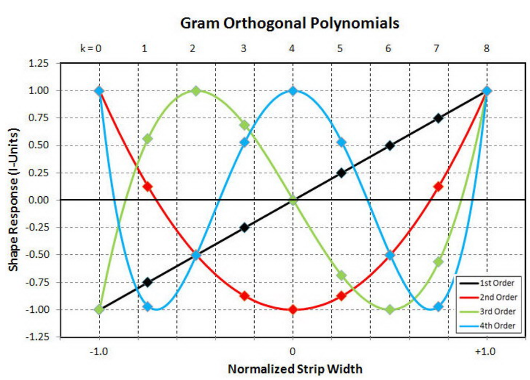

Figure 9 – Gram orthogonal polynomials.

$$P_0(y) = 1 \tag{13a}$$

$$P_1(y) = y \tag{13b}$$

$$P_i(y) = \frac{(M-1)(2i-1)}{i(M-i)} \, y \, P_{i-1}(y) - \frac{(i-1)(M-1+i)}{i(M-i)} P_{i-2}(y) \tag{13c}$$

for i = 2, 3, …Np

This polynomial basis method of approximation describes specific degrees of spatial curvature (in the Sobolev space) in monotonically increasing orders. The resulting coefficients, $\$_S^i$, provide a distribution / spectrum of spatial curvatures ingrained in the shape waveform pattern (this is a type of parameterization). This type of distribution is a kin to transformed descriptors like Frequency Responses and Bode Diagrams, and their relationships to a Time Response.

It is important to note that the 0th order polynomial, $P_0(y)$, is purposely exclude because it functions as a pure offset. By definition, ALL shape components must have a zero mean (across the transverse strip width). Any non-zero mean component would interact-with and therefore have to be absorbed by the Automatic Gauge Control system (AGC).

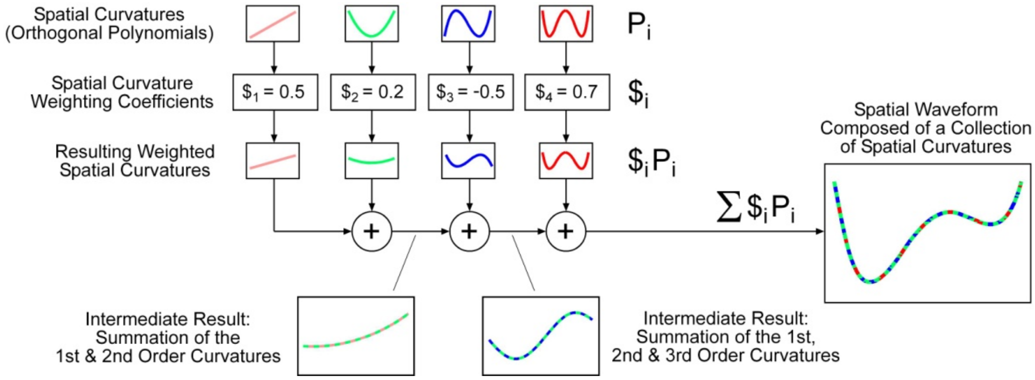

Figure 10 – Illustrations of the composition of a waveform from the weighted contributions of the Gram Polynomials (Eq(12)).

3.2 – Parametric Decomposition Using Orthogonal Polynomials

The vector collection, $\mathbf{\$}_S$, of the coefficients of Eq(12), provides a means of consolidating the parameterization of the describing spatial curvatures (forming a distribution / spectrum of curvature contributions).

$$\mathbf{\$}_S = \left[\$_S^1 \quad \$_S^2 \quad \cdots \quad \$_S^{N_p} \right]^T \tag{14}$$

The Gram polynomials form an orthogonal basis, which implies the coefficients, $\$_S^i$, can be determined through inner product methods, such that simple linear algebra can be used to perform this transformation. Over the discrete spatial sampling of y_M, and the inner product nature of Eq(12), a matrix transformation relationship is formed [15,16,17] from orthogonal polynomials evaluations:

$$\mathbf{S} = \tilde{\mathbf{P}}\mathbf{\$}_S \qquad \Leftrightarrow \qquad \mathbf{\$}_S = \left(\tilde{\mathbf{P}}^T\tilde{\mathbf{P}}\right)^{-1}\tilde{\mathbf{P}}^T\mathbf{S} = \tilde{\mathbf{P}}^T\mathbf{S} \qquad \Leftrightarrow \qquad \tilde{\mathbf{P}}^T\tilde{\mathbf{P}} = \mathbf{I}_{Np} \tag{15}$$

where the matrix $\tilde{\mathbf{P}}$ is the Curvature Decomposition Transform Matrix [15,16,17], and because of the polynomial orthogonality, the Inverse Transform Matrix is its transpose (as shown in the following):

$$\mathbf{P}(y_M) = \begin{bmatrix} P_1(y_M^0) & P_2(y_M^0) & \cdots & P_{Np}(y_M^0) \\ P_1(y_M^1) & P_2(y_M^1) & \cdots & P_{Np}(y_M^1) \\ \vdots & \vdots & \ddots & \vdots \\ P_1(y_M^{M-1}) & P_2(y_M^{M-1}) & \cdots & P_{Np}(y_M^{M-1}) \end{bmatrix} = \begin{bmatrix} \overline{\mathbf{P}_1} \\ \overline{\mathbf{P}_2} \\ \vdots \\ \overline{\mathbf{P}_{Np}} \end{bmatrix}^T \qquad \mathbf{P}_n = \mathrm{BlkDiag}\left(\left[\frac{1}{\sqrt{\overline{\mathbf{P}_1}^T\,\overline{\mathbf{P}_1}}} \quad \frac{1}{\sqrt{\overline{\mathbf{P}_2}^T\,\overline{\mathbf{P}_2}}} \quad \cdots \quad \frac{1}{\sqrt{\overline{\mathbf{P}_{Np}}^T\,\overline{\mathbf{P}_{Np}}}} \right]^T\right) \tag{16}$$

The orthogonality of the polynomials is not affected by scalar multiplication. Normalization is provided through the diagonal matrix, P_n. The Curvature Decomposition Transform Matrix is given by:

$$\tilde{\mathbf{P}}(y_M) = \mathbf{P}(y_M)\,\mathbf{P}_n \tag{17}$$

The parameter composition / decomposition process (method) of Eq(15) is illustrated in Figure 11.

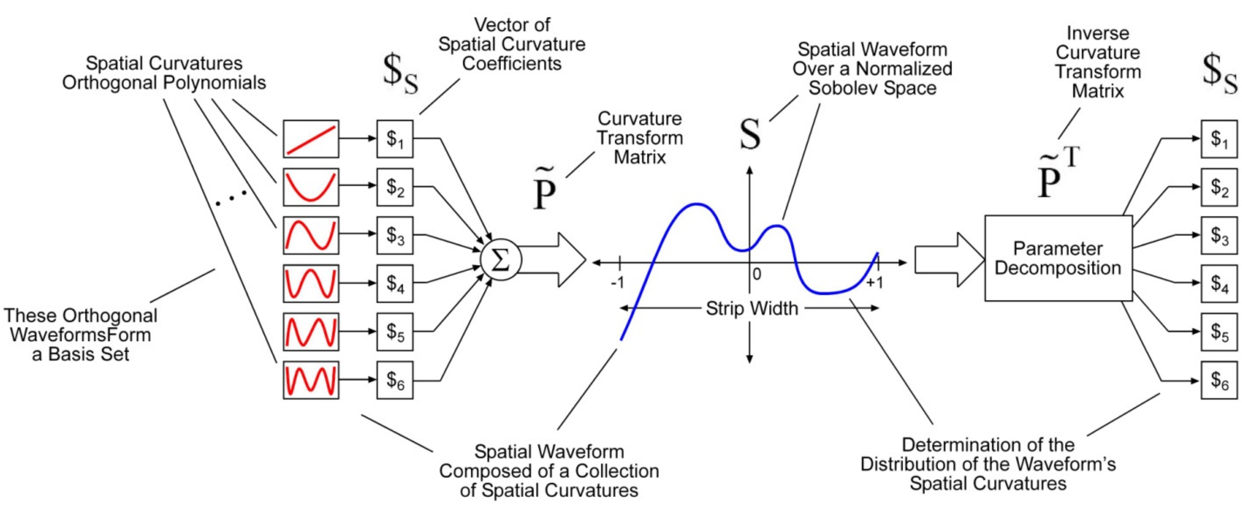

Figure 11 – Block diagram showing the parameter composition / decomposition process (method).

3.3 – A Coordinate Framework for Describing Spatial Curvature Content

The vector, $\$_S$, forms a distribution / spectrum of spatial curvatures that characterize the spatial waveform, **S**. As shown in Figure 12, it is possible to expand on the above method by forming a linearly independent, Cartesian coordinate system (associated with the nature of the orthogonal polynomials that form the decomposition), which uses the basis directions of the spatial curvature vector, $\$_S$.

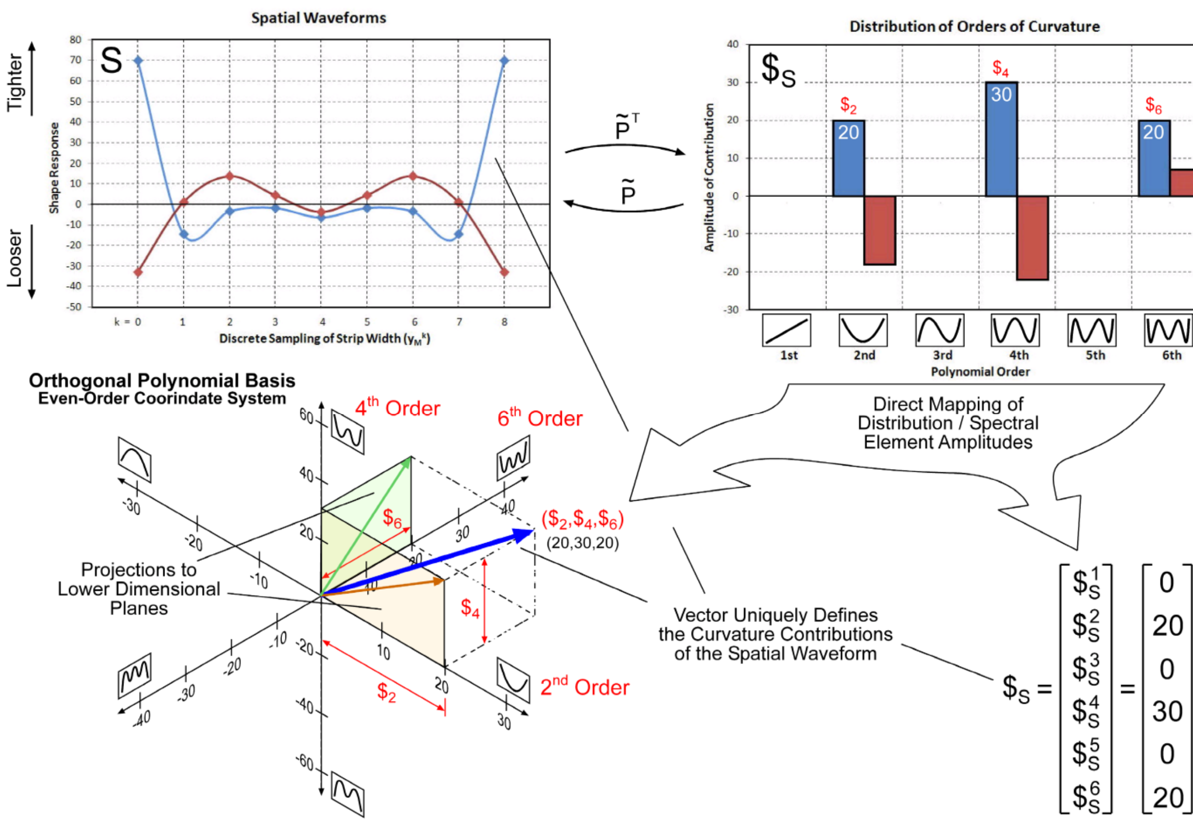

$$\$_S = \begin{bmatrix} \$_S^1 \\ \$_S^2 \\ \$_S^3 \\ \$_S^4 \\ \$_S^5 \\ \$_S^6 \end{bmatrix} = \begin{bmatrix} 0 \\ 20 \\ 0 \\ 30 \\ 0 \\ 20 \end{bmatrix}$$

Figure 12 – Illustration of the linearly independent Cartesian coordinate system formation and the associated mapping of a given spatial waveform's distribution / spectrum of spatial curvatures to form a single vector (point) within this linear space.

In Figure 12, the spatial waveform, **S**, is decomposed into its constituent curvature components, $\$_S$. This distribution / spectrum of spatial curvatures uniquely describes the spatial waveform, in terms of the contribution of each orthogonal polynomial needed to replicate the waveform. The resulting representation is a vector (point) within this Cartesian space, leading to a simplified means of characterizing the attributes of the spatial waveform. The location of a point within the Cartesian space defines the nature of its corresponding spatial waveform (a kin to determining the time response of a pole within the Laplacian phase plane). Figure 13 provides a "tour" of the waveform response characteristics (and associated strip shapes) for location within the coordinate system.

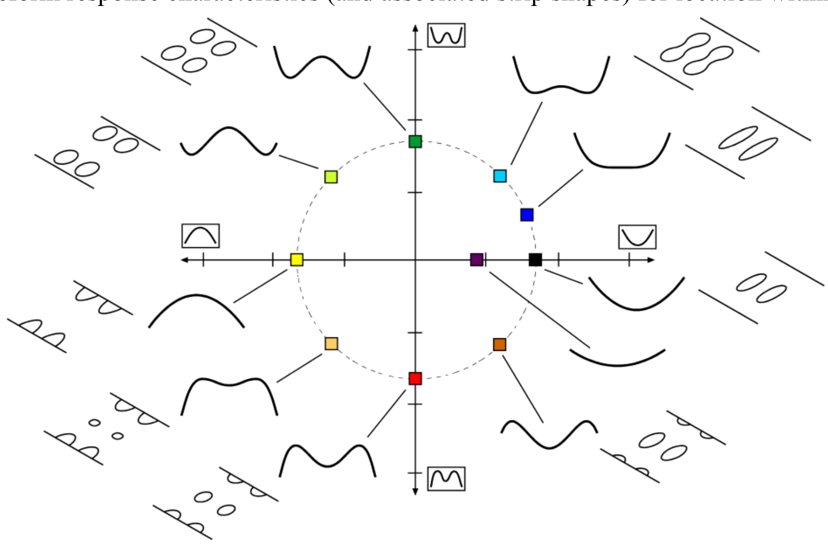

Figure 13 – Diagram showing the nature of a spatial waveform and the location of its corresponding spatial curvature distribution.

3.4 – Spatial Curvature Characteristics of the Rolled, Exit Shape

The spatial curvature distribution / spectrum of the rolled, exit shape is based on the waveform decomposition of the central relationships of Eq(1) and Eq(5) [15,16,17].

$$\mathbf{\$}_{\mathrm{T}} \subseteq \mathbf{\$}_{\mathrm{S}} = \mathbf{\$}_0 + \mathbf{\$}_{\mathrm{R}} + \mathbf{\$}_{\mathrm{A}} \tag{18a}$$

$$= \mathbf{\$}_0 + \mathbf{\$}_{\mathrm{R}} + \tilde{\mathbf{P}}^{\mathrm{T}} \mathbf{G}_{\mathrm{M}} \mathbf{A} \tag{18b}$$

where

- $\mathbf{\$}_{\mathrm{S}} \triangleq$ Rolled / exit strip shape's spatial curvature distribution / spectrum vector.
- $\mathbf{\$}_{\mathrm{T}} \triangleq$ Shape target's spatial curvature distribution / spectrum vector, indicating the desired curvatures.
- $\mathbf{\$}_{0} \triangleq$ Incoming strip shape's spatial curvature distribution / spectrum vector.
- $\mathbf{\$}_{\mathrm{R}} \triangleq$ Exit strip shape 's spatial curvature distribution / spectrum vector of the contributions formed by the natural mechanical deformation characteristics of the mill, and is based on a combination of material geometry and yield stress, applied separating force, roll cluster set-up of roll profiles and tapers, roll cluster flexibility [10], etc.. This component is static and can not be modified during on-line / rolling operations.
- $\mathbf{\$}_{\mathrm{A}} \triangleq$ Exit strip shape 's spatial curvature distribution / spectrum vector of the contributions induced by the top crown eccentrics and 1st IMR laterals, as transmitted / distributed to the roll bite through the roll cluster's mechanical characteristics (which function as a form of spatial filter). This component is dynamic and can be modified / adjusted during on-line / rolling operations. The nature of the actuation's spatial influence varies over the operating conditions, requiring a degree of adaptation to describe the full range of rolling conditions.

4.0 – DETERMINATION OF SPATIAL CURVATURE ENVELOPES

The orthogonal polynomial based coordinate framework of Section 3.3 provides a means of describing and coordinating the collection of spatial curvatures associated with a family of spatial waveform patterns. For a set / family of spatial waveform vectors, $\{\mathbf{S}\}$, through the parameter decomposition of, $\tilde{\mathbf{P}}^{\mathrm{T}}$,a corresponding set of spatial curvature spectra, $\{\mathbf{\$}_{\mathrm{S}}\}$, exists:

$$\{\mathbf{S}\} \Rightarrow \tilde{\mathbf{P}}^{\mathrm{T}} \Rightarrow \{\mathbf{\$}_{\mathrm{S}}\} \tag{19}$$

In the coordinate framework of Section 3.3, the set, $\{\mathbf{\$}_{\mathrm{S}}\}$, forms a grouping of points (an open set). These points populate a finite region, within this coordinate system framework, which can be over-contained by a closed surface / curve. This bounded closed surface is the Spatial Curvature Envelope for that specific set, $\{\mathbf{\$}_{\mathrm{S}}\}$.

4.1 – Accommodating the Shape Actuation Constraints

The exit / rolled strip shape spatial curvature spectrum of the constrained shape actuation is defined in [15,16], and is given by:

$$\mathbf{\$}_{\bar{\mathrm{A}}} = \tilde{\mathbf{P}}^{\mathrm{T}} \mathbf{G}_{\mathrm{M}} \bar{\mathbf{A}} \tag{20}$$

where $\bar{\mathbf{A}} \in \Re^{\mathrm{N}}$ is the constrained actuation vector. The full assortment of actuator constraints is described in [15,16,17].
For this examination, we will consider the following subset of top crown eccentric constraints:

<u>Stroke Limit</u> – To comply with the hydraulic cylinder's stroke and / or working range.

<u>Step Limit</u> – This provides compliance with the 1st order bending moment protection of the backing assembly bearings and shafts.

<u>Zero Mean</u> – To comply with the requirement that the crown actuation be non-interacting with the Automatic Gauge Control (AGC) system.

4.2 – Method of Determining the Bounding Spatial Curvature Envelope of the Constrained Shape Actuation

The basic process of determining the Bounding Spatial Curvature Envelope of $\mathbf{\$}_{\bar{\mathrm{A}}}$ involves the following steps:

1) Identify the set of ALL combinations of the constrained actuation, $\{\bar{\mathbf{A}}\}$, in terms of the constraints of Section 4.1.
2) Apply an individual constrained actuation setting to the mill shape model component, $\mathbf{G}_{\mathrm{M}}$, (based on the chosen conditions and operating point) to obtain the associated shape waveform, $\mathbf{S}_{\bar{\mathrm{A}}}$.
3) Decompose the resulting shape waveform to its associated spatial curvature spectrum vector, $\mathbf{\$}_{\bar{\mathrm{A}}}$, (or evaluation of Eq(20)).
4) Map the resulting spectral data (vector) within the curvature coordinate framework of Section 3.3 (i.e., a point is plotted for each actuator setting).

These steps provide the ability to plot a single point, for each instance of the actuator settings, within the coordinate framework. As the actuator settings are varied over their entire constrained range, $\{\bar{\mathbf{A}}\}$, a collection of points develops, $\{\$_{\bar{A}}\}$. The linear algebraic nature of the model, $\mathbf{G}_M$, and parameter decomposition of Eq(20) provides a convenient method of performing an exhaustive survey of the family of actuator settings, with relatively low computational effort. The grouping of points maps-out / fills-in a finite region of the curvature space (an open set). This region can be bounded by an over-containing, closed surface / curve that forms the spatial curvature envelope for the set $\{\$_{\bar{A}}\}$. This is the SACE for that specific condition / operating point. Figure 14 provides a flow chart and illustration of this process.

The nature of the closed surface / curve of the spatial curvature envelope is evaluated using multi-dimensional edge / extremity locating image processing techniques [4]. The determined extremities are interconnected by a multivariate interpolation method [4,20] that assures a complete over-containment of region's plotted points.

It is possible to simplify this approach by projecting the mapped points to a lower dimensional surface (e.g., the 2nd / 4th order plane shown in Figure 12). This strategy provides a more practical (understandable) depiction of the envelope, but when evaluating the results, one must be cognizant of the influence of the "unseen" higher dimensional content.

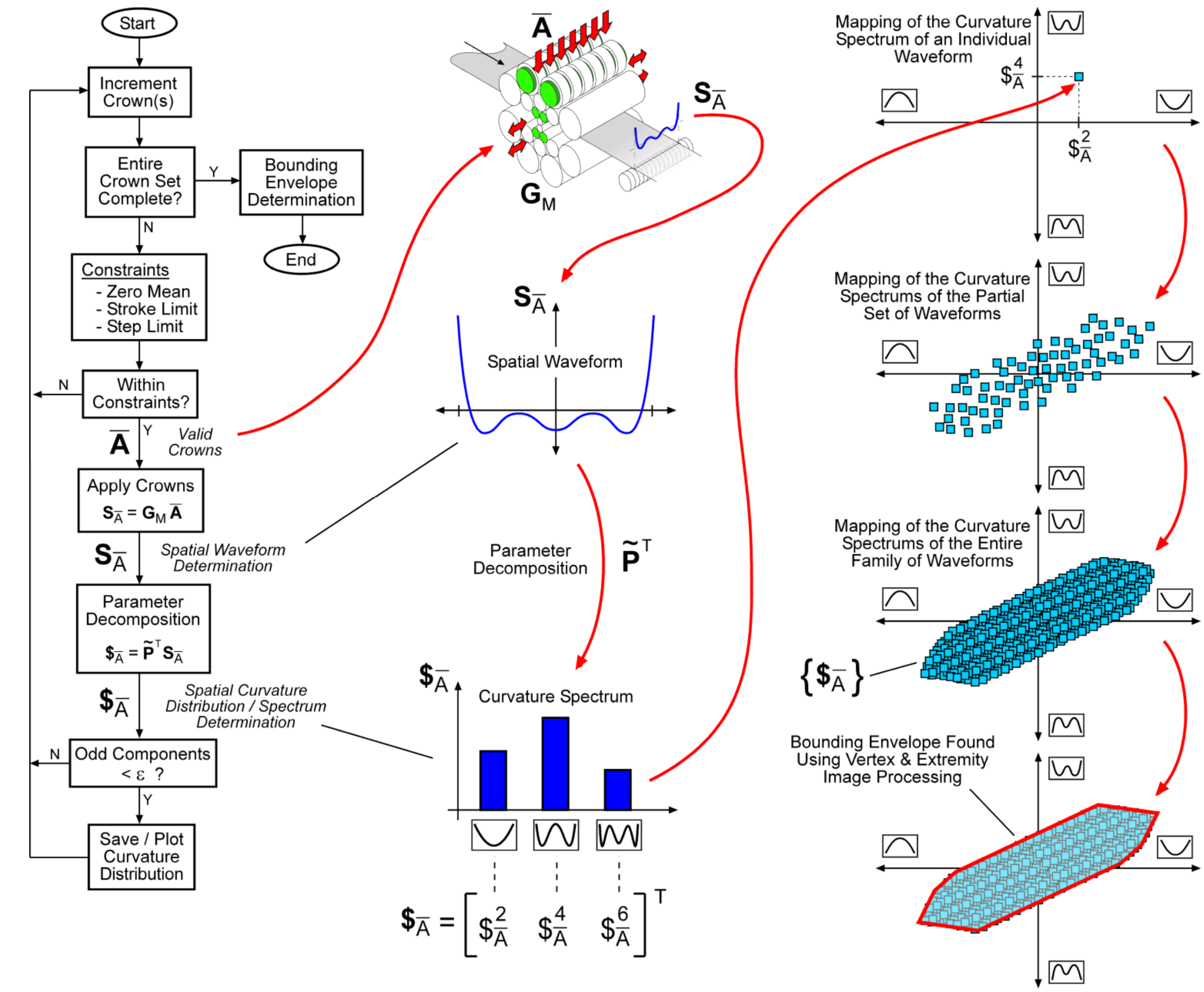

Figure 14 – Process of determining the bounding spatial curvature envelope (SACE) associated with the family of transverse shape waveforms generated by the full range of the constrained shape actuation.

It is important to note the scale of the data generated by this approach. If one considers the pattern of applied top crown eccentric settings, having an incremental resolution of 1% (over the range of +/-100% for each actuator), the set {A} contains just over 1.33 x 10^{16} (i.e., 201^7) different combinations of actuator settings, for a classical 7 top crown arrangement. Depending on the nature of the applied constraints, the set $\{\bar{\mathbf{A}}\}$ can be substantially smaller (on the order of several thousands to tens of thousands – which is still a large data set to work with). Fortunately, the compact linear algebraic arrangement of Eq(20) provides a computationally efficient framework for determining even the worst case actuation constraints and envelope conditions.

CONCLUSION

This paper has examined a procedural method of characterizing the Shape Actuator Capabilities Envelopes (SACE) of 20-high cluster mills. This approach decomposes the complexities of the rolled shape's spatial waveform ((transverse stress pattern across the strip) resulting from a given shape actuator system setting, into its simplified curvature constituents (a collection of ordered spatial curvatures). The parameter decomposition is based on an orthogonal polynomial framework (vector space), whose basis set consists of the directions associated with the fundamental curvatures (1^{st}, 2^{nd}, 3^{rd}, etc. orders of spatial curvature). For a specific shape actuator setting, the resulting shape waveform is composed of a weighted collection of curvatures that form a point (described by a unique vector) in the vector space. By evaluating the rolled shape curvatures over the entire range of shape actuator settings (including the presence of physical and operational constraints), the resulting points (vectors) map-out an open region in the space. This region indicates the extent of the corrections that the shape actuators can provide (for a given situation involving the incoming shape and roll cluster deformation characteristics). The SACE is determined by forming a bounding, piece-wise continuous, closed surface along the extremities of the collection of plotted points / vectors (the SACE surface over-contains the group of plotted points).

REFERENCES

1 Hata, K, et al., "Universal Crown Control Mills", Hitachi Review, Vol. 34, No. 4, 1985, pp 168-174.

2 Ginzburg, V.B., *Fundamentals of Flat Rolling*, Marcel Dekker, Inc., New York, NY, 2000, pp 819-820.

3 Zipf, M.E., "20-High Cluster Mill Shape Actuator Characterization through Parameter Identification Methods", Proceedings of the Associação Brasileira de Metalurgia e Materiais, 47th Rolling Seminar – Processes, Rolled and Coated Products, October 26-29, 2010, Belo Horizonte, MG, Brazil.

4 Hall, E.L., *Computer Image Processing and Recognition*, Academic Press, New York, NY, 1979, pp 390-412.

5 Duprez, J.L. and Turley, J.W., *The Sendzimir Manual*, Waterbury, CT : T. Sendzimir, Inc. / Jean-Louis Duprez Publications, 2000.

6 Grimble, M.J., Fotakis, J., "The Design of Strip Shape Control Systems for Sendzimir Mills", IEEE Transactions on Automatic Control, Vol. AC-27, No. 3, pp 656-666, June 1982.

7 Ringwood, J.V., Grimble, M.J., "Shape Control in Sendzimir Mills Using Both Crown and Intermediate Roll Actuators", IEEE Transactions on Automatic Control, Vol. 35, No. 4, pp 453-459, April 1990.

8 Ringwood, J.V., "Shape Control Systems for Sendzimir Steel Mills", IEEE Transactions on Control System Technology, Vol. 8, No. 1, pp 70-86, January, 2000.

9 Zipf, M.E., C.K. Godwin and D.R. Wisti, "Modeling and Simulation of Sendzimir Mill Shape Control Actuation Sensitivities and Capabilities Envelope with Applications to Multivariable Shape Control", Proceedings of the Associação Brasileira de Metalurgia e Materiais, 43rd Rolling Seminar – Processes, Rolled and Coated Products, October 17-20, 2006, Curitiba, PR, Brazil, Compact Disk (CD) pp 856-866.

10 Zipf, M.E., Godwin, C.K. and Wisti, D.R., "Comparative Studies of Sendzimir Mill Shape Control Responses", Proceedings of the 2008 AISTech Annual Conference, Pittsburgh, PA, May 5-8, 2008, Association of Iron and Steel Technologies, Pittsburgh, PA. and Omnipress, Madison, WI., 2008 Compact Disc (CD).

11 Zipf, M.E., "20-High Cluster Mill Shape Actuator Characterization through Parameter Identification Methods", Proceedings of the Associação Brasileira de Metalurgia e Materiais, 47th Rolling Seminar – Processes, Rolled and Coated Products, October 26-29, 2010, Belo Horizonte, MG, Brazil.

12 Gunawardene, G.W.D.M., "Static Model Development for the Sendzimir Cold Rolling Mill", Ph.D. Dissertation, Sheffield City Polytechnic, 1982.

13 Guo, R.M., Malik, A., "Development of New Crown / Shape Control Model for Cluster Mills", AIST Conference Proceedings, Nashville, 2004.

14 Malik, A.S., Grandhi, R.V., Zipf, M.E., "Optimal Cluster Mill Pass Scheduling With an Accurate and Rapid New Strip Crown Model", Proceedings of the NUMIFORM '07, the 9th International Conference on Materials Processing and Design: Modeling, Simulation and Applications, June 17-21, 2007, Proto, Portugal, American Institue of Physics, pp 1041-1046.

15 Zipf, M.E. and Godwin, C.K., Reachability Conditions of Shape Targets in 20-High Cluster Mills, Proceedings of the 2011 AISTech Annual Conference, Indianapolis, IN, May 2-5, 2011, Association of Iron and Steel Technologies, Pittsburgh, PA and Omnipress, Madison, WI, 2011 Compact Disc (CD).

16 Zipf, M.E. and Godwin, C.K., Shape Correction Capabilities Envelopes of 20-High Cluster Mills, Proceedings of the 4th International Conference on Modeling and Simulation of Metallurgical Processes in Steelmaking (STEELSIM), Dusseldorf, Germany, June 27 – July 1, 2011, METEC InSteelCon 2011, TEMA Technologie Marketing AG, Aachen, Germany, 2011 Compact Disc (CD).

17 Zipf, M.E., "Characterization of the Restrictions in Shape Adjustment Capabilities Associated with Actuator Constraints", Proceedings of the Associação Brasileira de Metalurgia e Materiais, 48th Rolling Seminar – Processes, Rolled and Coated Products, October 24-27, 2011, Santos, Brazil.

18 Timan, A.F., *Theory of approximation of functions of a real variable*, Dover Publications, Inc., Mineola, NY, 1963

19 Kristinsson, K. and Dumont, G.A., "Cross-directional Control on Paper Machines using Gram Polynomials", Automatia, Vol. 32, No. 4, pp. 533-548, 1996.

20 Press, W.H., Flannery, B.P., Teukolsky, S.A. and Vetterling, W.T., *Numerical Recipes : The Art of Scientific Computing*, Cambridge University Press, New York, NY, 1986.

21 Zipf, M.E., "Multivariable Directions in the Improvement of Shape Actuator Performance", Proceedings of the 2012 AISTech Annual Conference, Atlanta, GA, May 7-10, 2012, Association of Iron and Steel Technologies, Pittsburgh, PA. and Omnipress, Madison, WI., 2012 Compact Disc (CD).